

## Toughening of highly translucent zirconia by monoclinic ZrO<sub>2</sub> and SiO<sub>2</sub> particle coating

Soichiro UNO<sup>1,2</sup>, Masahiro OKADA<sup>1</sup>, Hiroaki TAKETA<sup>1,2</sup>, Yasuhiro TORII<sup>2</sup> and Takuya MATSUMOTO<sup>1</sup>

<sup>1</sup>Department of Biomaterials, Graduate School of Medicine, Dentistry and Pharmaceutical Sciences, Okayama University, 2-5-1 Shikata-cho, Kita-ku, Okayama 700-8558, Japan

<sup>2</sup>Department of Comprehensive Dentistry, Graduate School of Medicine, Dentistry and Pharmaceutical Sciences, Okayama University, 2-5-1 Shikata-cho, Kita-ku, Okayama 700-8558, Japan

Corresponding author, Takuya MATSUMOTO; E-mail: tmatsu@md.okayama-u.ac.jp

The mechanical properties of highly translucent partially stabilized zirconia (PSZ) need to be improved; however, improvement of mechanical properties often decreases translucency. To overcome this problem, a monoclinic ZrO<sub>2</sub> (mZrO<sub>2</sub>)/SiO<sub>2</sub> dispersion was prepared and applied as a coating material for PSZ. The influence of surface treatment by the mZrO<sub>2</sub>/SiO<sub>2</sub> dispersion on the surface topography, crystallography, and mechanical properties of highly translucent PSZ was investigated in this study. Following the treatment, the mechanical strength of highly translucent PSZ improved by 170% compared with control, for the best mZrO<sub>2</sub>/SiO<sub>2</sub> dispersion ratio and heating temperature condition, while maintaining its translucency. The proposed coating is promising for improving the mechanical properties of highly translucent PSZ.

**Keywords:** Highly translucent partially stabilized zirconia, Monoclinic phase, Biaxial flexural strength, Thermal treatment

### INTRODUCTION

Ceramic restorations are in high demand in the field of dentistry, owing to their high esthetics and biocompatibility that allows to avoid metal allergy. Among ceramic materials, zirconia has received the most attention, owing to its good mechanical strength<sup>1,2</sup>.

Zirconia can exist in three crystal phases: monoclinic, tetragonal, and cubic. When non-stabilized zirconia is heated above its phase transition temperature and cooled back to room temperature, its crystal structure is transformed from the tetragonal to the monoclinic phase, accompanied by a 3–4% volume expansion, leading to easy degradation of zirconia. Addition of yttria (Y<sub>2</sub>O<sub>3</sub>) avoids this crystal phase transformation and makes the material thermodynamically metastable; this material is called yttria-stabilized tetragonal zirconia polycrystal (Y-TZP)<sup>3</sup>. Conventional Y-TZP (stabilized with *ca.* 3 mol% Y<sub>2</sub>O<sub>3</sub>) exhibits very good mechanical strength, because when a crack is formed on its surface, the crystal phase around the crack transforms from tetragonal to monoclinic (tetragonal-monoclinic transition). This tetragonal-monoclinic transition prohibits crack growth and breaking<sup>3,4</sup>. However, owing to the nature of tetragonal zirconia (tZrO<sub>2</sub>) and the presence of alumina (Al<sub>2</sub>O<sub>3</sub>) as a sintering agent<sup>5</sup>, conventional Y-TZP has low translucency.

Highly translucent partially stabilized zirconia (PSZ) was developed for overcoming this problem; the phase composition of this novel material is different from that of conventional Y-TZP<sup>6,7</sup>. Owing to a higher Y<sub>2</sub>O<sub>3</sub> stabilizer content, this highly translucent zirconia

contains a significant amount of cubic zirconia (cZrO<sub>2</sub>) and a smaller amount of Al<sub>2</sub>O<sub>3</sub>, rendering this zirconia more translucent. Moreover, such highly translucent zirconia ceramics are hydrothermally stable, because cZrO<sub>2</sub> grains do not transform to the monoclinic zirconia (mZrO<sub>2</sub>). A large amount of cZrO<sub>2</sub>, on the other hand, results in a decrease in mechanical properties, especially in terms of strength and fracture toughness<sup>7</sup>.

In previous studies, the mechanical strength of highly translucent zirconia was improved by adding other oxides<sup>8,9</sup>. In addition, infiltrating glass ceramics was also considered for this purpose<sup>10</sup>. Although these approaches are valuable, improvement is not sufficient for maintaining the material's translucency. Therefore, easier handling and more economical methods are required.

In this study, we attempted to increase the mechanical strength of highly translucent PSZ while maintaining its translucency; we used surface coating, the motivation for which was the toughening mechanism of strengthened glass, where the outer surface is compressed for avoiding breakage owing to the outside stress. We used a dispersion containing mZrO<sub>2</sub> and SiO<sub>2</sub> as a coating agent for PSZ. The mZrO<sub>2</sub> works to form a compressive stress layer on the material's surface using volume change, when the crystal phase changed from tetragonal to monoclinic phase. The SiO<sub>2</sub> serves as a binder to improve wettability and to accelerate the sintering of mZrO<sub>2</sub>. In addition, both mZrO<sub>2</sub> and SiO<sub>2</sub> have smaller thermal expansion coefficients than the base PSZ material<sup>11,12</sup>, which also supports formation of a compressive stress layer on the material's surface.

Color figures can be viewed in the online issue, which is available at J-STAGE.

Received Dec 14, 2018; Accepted Apr 22, 2019

doi:10.4012/dmj.2018-415 JOI JST.JSTAGE/dmj/2018-415

## MATERIALS AND METHODS

### Materials

Pre-sintered PSZ (Katana UTML) was kindly supplied by Kuraray Noritake Dental (Tokyo, Japan). Alumina particles (size, 50  $\mu\text{m}$ ) (Hi-Aluminas; Shofu, Kyoto, Japan) were used for sandblasting. The crystal composition of as-sintered Katana UTML is reported as follows:  $\text{cZrO}_2$  70.6 wt%;  $\text{tZrO}_2$  28.9 wt%;  $\text{mZrO}_2$  0.2 wt%; rhombohedral zirconia ( $\text{rZrO}_2$ ) 0.3 wt%<sup>7</sup>. The  $\text{mZrO}_2$  crystals (particle size, 13 nm) were prepared by a hydrothermal treatment of a 4 mol/L  $\text{ZrOCl}_2$  (Wako Pure Chemical Industries, Osaka, Japan) aqueous solution at 200°C<sup>13,14</sup>. The  $\text{mZrO}_2$  crystals were centrifugally washed with ultrapure water, dried in air, and then re-dispersed in ultrapure water (solid content, 50 wt%). Milli-Q water (Millipore, Bedford, MA, USA) with a specific resistance of  $18.2 \times 10^6 \Omega \cdot \text{cm}$  was used to prepare and to disperse the  $\text{mZrO}_2$  crystals. An aqueous suspension of 50 wt%  $\text{SiO}_2$  stabilized by  $\text{Na}_2\text{O}$  (LUDOX® TM-50, Sigma-Aldrich, St. Louis, MO, USA) was used for the component of coating. A dispersion for the coating of PSZ was made by mixing the two components and diluting into 25 wt% solid content by ultrapure water, and then sonicating them with an ultrasonic bath (ASU-2D; AS ONE, Osaka, Japan) for 10 min at 23 kHz, to obtain the dispersion.

### Sample preparation

A low-speed cutting machine was used to cut the pre-sintered zirconia under a wet condition with tap water. After the disks were sintered at 1,550°C for 2 h (heating rate: 10 °C/min from room temperature to 1,550°C; cooling rate: below 10 °C/min), the sintered PSZ (~14 mm in diameter and ~1.2 mm in thickness) were subjected to the following treatment procedures (Fig. 1):

- 1) Sandblasting: Both sides of the as-sintered disk were ground under the wet condition, using a rotator fixed with a coarse diamond grinding disk (Apex CGD 125  $\mu\text{m}$ ; Buehler, Illinois Tool Works, Chicago, IL, USA) followed by grinding using P600 and P1000 silicon carbide abrasive papers (Nihon Kenshi, Hiroshima, Japan). Then, the single-side of the disk after grinding was sandblasted with 50  $\mu\text{m}$  alumina particles, using a laboratory sandblaster (Hi-Blaster III; Shofu) at 0.2 MPa for 10 s. After the sandblasting, each disk was cleaned with ultrapure water three times, using an ultrasonic cleaner (ASU-2D) at 23 kHz for 1 min, to remove the alumina particles

and debris.

- 2) Surface coating: A drop (10  $\mu\text{L}$ ) of the  $\text{mZrO}_2/\text{SiO}_2$  dispersion ( $\text{mZrO}_2/\text{SiO}_2$  weight ratio: 20/1, 10/1, 8/3, or 6/5) was applied on the sandblasted side of the disk, and then dried using mild air blowing.
- 3) Heating treatment: The  $\text{mZrO}_2/\text{SiO}_2$ -coated samples were heated in a calcination furnace (KBF314, Koyo Thermo Systems, Nara, Japan) at three different temperatures (1,000, 1,300, and 1,500°C) for 2 h (heating rate: 10°C/min; cooling rate: <10°C/min).

In this study, the  $\text{mZrO}_2/\text{SiO}_2$ -coated PSZ treated at different heating temperatures (1,000, 1,300, or 1,500°C) was prepared at a constant  $\text{mZrO}_2/\text{SiO}_2$  ratio of 10/1 to evaluate the effect of heating temperature. The  $\text{mZrO}_2/\text{SiO}_2$ -coated PSZ treated at different  $\text{mZrO}_2/\text{SiO}_2$  weight ratio (20/1, 10/1, 8/3, or 6/5) was also prepared at a heating temperature of 1,500°C, to evaluate the effect of  $\text{mZrO}_2/\text{SiO}_2$  dispersion composition.

### Mechanical strength measurements

The mechanical strength of samples was measured by a biaxial flexural strength test ( $n=5$ ), which was performed using the piston-on-three ball technique<sup>15</sup> in a universal testing machine (Autograph AG-X, Shimadzu, Kyoto, Japan). Three 3.2-mm-diameter stainless steel balls that were equidistant from each other were placed on a circle (diameter, 10 mm). The disk was placed centrally on the steel balls. The sandblasted side was faced on the steel balls, where a load piston (diameter, 1.2 mm) was applied from the opposite side of the sandblasted surface (crosshead speed, 1.0 mm/min), to apply a tensile stress on the sandblasted side. The fracture load for each specimen was recorded and the biaxial flexural strength was calculated using the following equation:

$$S = \frac{-0.2387P(X-Y)}{d^2}$$

where  $S$  is the biaxial flexural strength (MPa);  $P$  is the fracture load (N); and  $d$  is the specimen disk thickness at the fracture origin (mm).  $X$  and  $Y$  were determined as follows:

$$X = (1+u) \ln \left( \frac{r_2}{r_3} \right)^2 + \left[ \frac{1-u}{2} \right] \left( \frac{r_2}{r_3} \right)^2$$

$$Y = (1+u) \left[ 1 + \ln \left( \frac{r_1}{r_3} \right)^2 \right] + (1-u) \left( \frac{r_1}{r_3} \right)^2$$

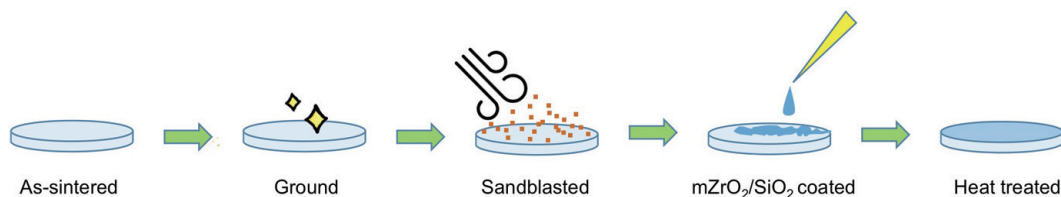


Fig. 1 The experimental flow of surface treatment.

where  $u$  is Poisson's ratio (0.25),  $r_1$  is the radius of the support circle,  $r_2$  is the radius of the load piston, and  $r_3$  is the radius of the sample.

#### Surface observation and analysis

Surface morphology was observed by scanning electron microscopy (SEM), using a JSM-6701F microscope (JEOL, Tokyo, Japan) operated at 5 kV, after all of the samples were fixed on an aluminum stub and coated with osmium using an osmium coater Neoc-Pro (Meiwafosis, Tokyo, Japan). Elemental analysis was performed by scanning electron microscopy-energy dispersive spectroscopy (SEM-EDS), using a H4800 microscope (Hitachi High Technology, Tokyo, Japan) operated at 15 kV, after all of the samples were fixed on an aluminum stub and osmium coating.

The crystal phases of the samples were determined by measuring the samples' X-ray diffraction (XRD) patterns. The XRD data were collected from 20° to 40° at a scan speed of 2°/min, using a  $\theta/2\theta$  diffractometer (RINT 2500HF, Riken, Osaka, Japan), using Cu-K $\alpha$  (1.54 Å) irradiation at 40 kV and 200 mA.

#### Translucency of treated samples

Transparency parameter of the treated samples (mZrO<sub>2</sub>/SiO<sub>2</sub> weight ratio=10/1; treatment temperature=1,500°C) was compared with the control sample without treatment ( $n=5$ ). The spectral reflectance of the sample was measured against white ( $L^*=96.7$ ,  $a^*=-0.1$  and  $b^*=-0.3$ ) or black ( $L^*=1.2$ ,  $a^*=-0.3$  and  $b^*=-0.1$ ) ceramic tile background, using a spectrophotometer (CM-3600d, Konica Minolta, Tokyo, Japan). A hydrocarbon oil (pentadecane; refractive index  $n_D=1.43$ ) was used to contact between the treated sample surfaces and the backgrounds. Translucency parameter (TP) values were determined by calculating the difference between the color components of the same specimen on the black

and white backgrounds, according to the following formula<sup>16,17</sup>:

$$TP=[(L_B^*-L_W^*)^2+(a_B^*-a_W^*)^2+(b_B^*-b_W^*)^2]^{1/2}$$

where  $L^*$ ,  $a^*$  and  $b^*$  are the lightness, green-red and blue-yellow components, respectively; and the subscripts  $B$  and  $W$  refer to the color components over a black and white background, respectively.

#### Statistical analysis

A nonparametric Steel-Dwass test was performed to investigate the effect of heat treatment temperature or solution composition (mZrO<sub>2</sub>/SiO<sub>2</sub> weight ratio) on biaxial flexural strength ( $n=5$ ). A nonparametric Welch's  $t$  test was performed to investigate the change in the translucency parameters ( $n=5$ ). All statistical tests were performed using R version 3.3.2 (R Foundation for Statistical Computing, Vienna, Austria), with a significance level of 0.05.

## RESULTS

#### Effect of heating temperature

To understand the effect of heating temperature on the mZrO<sub>2</sub>/SiO<sub>2</sub>-coated PSZ, the biaxial flexural strength test was conducted at a constant mZrO<sub>2</sub>/SiO<sub>2</sub> ratio of 10/1. The results indicated that the mechanical strength did not change significantly after 1,000 or 1,300°C treatment, whereas the strength significantly increased after 1,500°C treatment, compared with as-sintered samples. The sample heated at 1,000°C exhibited the strength of 440 MPa, while the sample heated at 1,500°C exhibited the strength of 725 MPa (Fig. 2a).

To understand the crystal phases of the samples, XRD analysis was conducted. The results indicated that the heated samples exhibited a combination of the

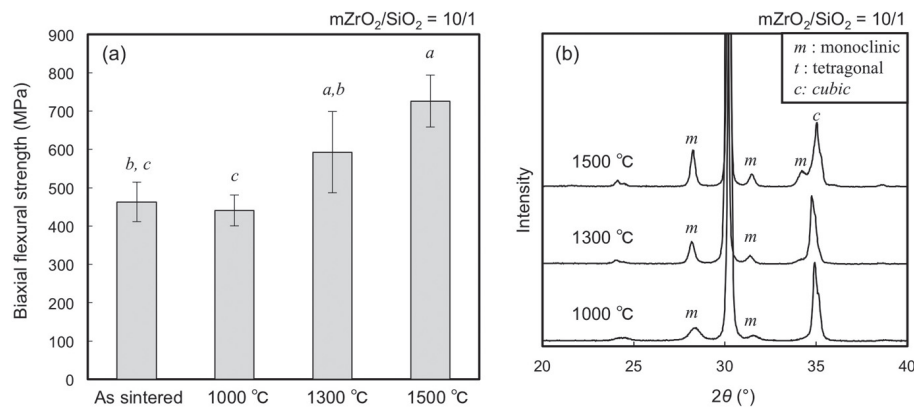


Fig. 2 Effects of heat temperature on (a) mechanical strength and (b) crystal phase of samples.

The sandblasted PSZ disks were coated with mZrO<sub>2</sub>/SiO<sub>2</sub> (10/1, w/w) and heat treated at different temperatures. Different italic letters on the bars in the graph (a) indicate statistically significant difference from Steel-Dwass test ( $p<0.05$ ,  $n=5$ ).

monoclinic phase (derived from the coated layer) and the cubic phase (derived from the PSZ substrate); the peak attributed to the monoclinic phase became sharper as the treatment temperature increased, suggesting the crystal growth (and sintering) of  $mZrO_2$  (Fig. 2b).

#### Effect of dispersion composition

Next, to understand the effect of the  $mZrO_2/SiO_2$  dispersion composition on the PSZ coatings, the biaxial flexural strength test was conducted at a constant heating temperature of 1,500°C. The results indicated that the mechanical strength did not significantly change at the highest (20/1) and the lowest (6/5)  $mZrO_2/SiO_2$  weight ratio, whereas those increased at the  $mZrO_2/SiO_2$  weight

ratios of 10/1 and 8/3, compared with the as-sintered PSZ. The maximal mechanical strength was 725 MPa (Fig. 3a). In addition, XRD analysis was conducted. The results indicated a reduced presence of the monoclinic phase and an increase in the presence of both the cubic and tetragonal phases of the crystals, with increasing  $SiO_2$  ratio (Fig. 3b). Of note, the  $ZrSiO_x$  phase was not detected in any of the XRD patterns at any of the  $mZrO_2/SiO_2$  ratios in this study.

#### Observations of surfaces using different modification methods

To understand the surface properties caused by the surface treatment, SEM observations were conducted.

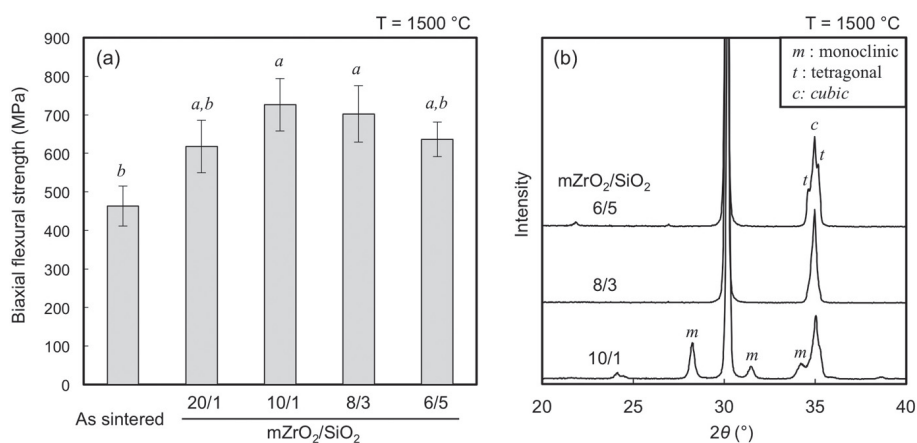


Fig. 3 Effects of dispersion composition on (a) mechanical strength and (b) crystal phase of samples.

The sandblasted PSZ disks were coated with  $mZrO_2/SiO_2$  and heat treated at 1,500°C. Different italic letters on the bars in the graph (a) indicate statistically significant difference from Steel-Dwass test ( $p < 0.05$ ,  $n = 5$ ).

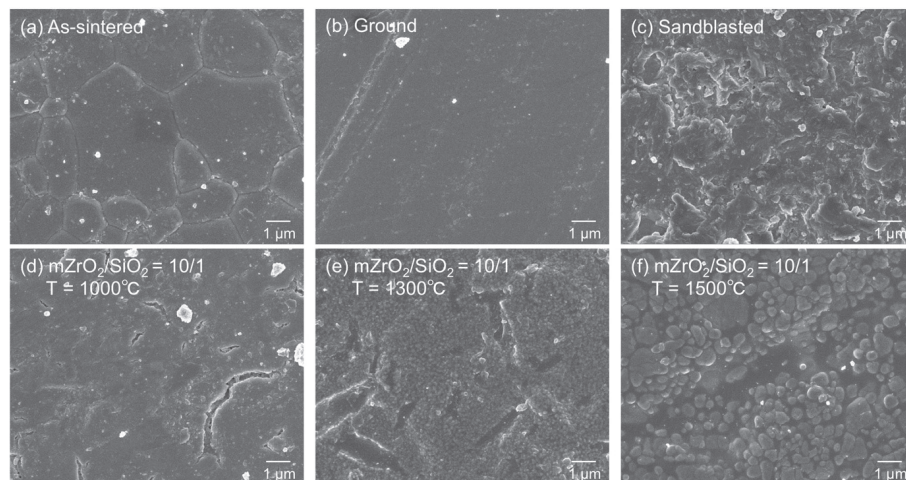


Fig. 4 SEM images of (a) as-sintered, (b) ground, (c) sandblasted and (d–f)  $mZrO_2/SiO_2$  (10/1, w/w) coated PSZ after heating at different temperatures (°C): (d) 1,000, (e) 1,300, and (f) 1,500.

The results indicated that the as-sintered-, ground-, and sandblasted- surfaces featured no cracks on the samples' surfaces; however, some tiny cracks, which were formed by drying the  $m\text{ZrO}_2/\text{SiO}_2$  dispersion on the PSZ, remained on the surface that was heated at  $1,000^\circ\text{C}$ . The surface of the sample heated at  $1,300^\circ\text{C}$  was covered with granule-like newly formed crystals, and the cracks were filled with amorphous phase. The size of granule-like crystals increased for the samples heated at  $1,500^\circ\text{C}$ . Apparently, tiny crystals fused to form larger ones (Fig. 4).

#### Surface heated at $1,500^\circ\text{C}$ , for different $m\text{ZrO}_2/\text{SiO}_2$ ratios

Altogether, the  $m\text{ZrO}_2/\text{SiO}_2$ -coated samples heated at  $1,500^\circ\text{C}$  exhibited improved mechanical strength; in addition, the mechanical strength of the samples also depended on the  $m\text{ZrO}_2/\text{SiO}_2$  ratio. To further understand the dependence of surface properties on coating at different  $m\text{ZrO}_2/\text{SiO}_2$  ratios, elemental analysis was conducted using EDS. The surface of the

$m\text{ZrO}_2/\text{SiO}_2=20/1(\text{w/w})$  sample exhibited an “island-sea structure”, with the islands consisting of densely packed granule-like crystals, while the sea was dried (*i.e.*, the PSZ substrate surface was exposed). With increasing  $\text{SiO}_2$  content, the space between granule-like crystals in the island regions became larger. Interestingly, elemental mapping of Si and Zr indicated the specific distribution of each element on the sample's surface. Here,  $\text{ZrO}_2$  was located mainly in the island regions, while  $\text{SiO}_2$  was located mainly in the sea surrounding the island regions on the surface (Fig. 5). Note that the gaps between the island  $\text{ZrO}_2$  regions were not filled with  $\text{SiO}_2$  at  $m\text{ZrO}_2/\text{SiO}_2=20/1(\text{w/w})$ , whereas the gaps filled with  $\text{SiO}_2$  at or below  $m\text{ZrO}_2/\text{SiO}_2=10/1(\text{w/w})$ .

#### Translucency of samples after surface treatment

To confirm the effect of surface treatment on the translucency of zirconia samples, translucency parameters were compared. The results of this analysis indicated that the samples' surfaces did not change their translucency after treating the samples (Fig. 6).

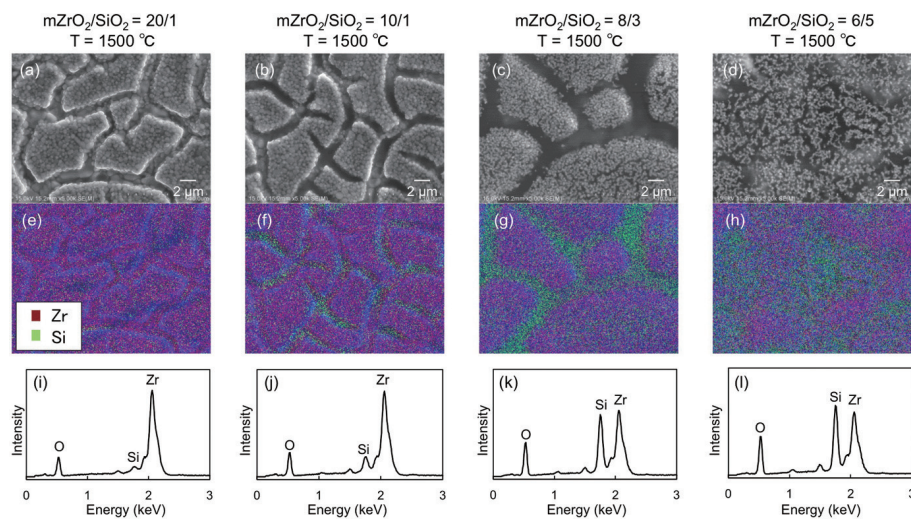


Fig. 5 (a–d) SEM images, (e–h) Zr and Si elemental mapping and (i–l) EDS spectra of samples coated with  $m\text{ZrO}_2/\text{SiO}_2$  and heat treated at  $1,500^\circ\text{C}$ .

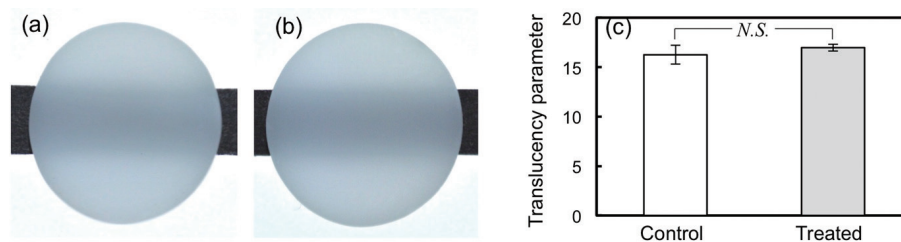


Fig. 6 Digital photographs of (a) control and (b) the  $m\text{ZrO}_2/\text{SiO}_2$  (10/1, w/w)-coated sample after heating at  $1,500^\circ\text{C}$ , showing the translucency. (c) Quantitative results of translucency parameters. N.S. in the graph (c) indicates no significant difference from Welch's t test ( $p>0.05$ ,  $n=5$ ).

## DISCUSSION

The mechanical properties of highly translucent PSZ require improvement; however, improvement of mechanical properties often negatively affects the materials' translucency. In general, it is known that temperatures above 1,000°C are sufficient for grazing of zirconia ceramics (850–950°C<sup>18</sup>). This glazing also contributes to the re-crystallization of zirconia surface<sup>19,20</sup>. Thus, our hypothesis was that adjustment of the glazing (coating) material can improve the mechanical properties of PSZ through the re-crystallization process. For this purpose, we decided to use mZrO<sub>2</sub> as a main coating material. Although mZrO<sub>2</sub> largely affects the mechanical strength of the base substrate, its surface binding affinity is relatively weak. Therefore, SiO<sub>2</sub> was added to the coating solution as a binder. Thus, in the present study we investigated the influence of surface treatment by mZrO<sub>2</sub>/SiO<sub>2</sub> dispersion on the surface topography, crystallography, and mechanical properties of highly translucent PSZ. Although Venkatesh *et al.* reported the mixing of nanosized ZrO<sub>2</sub> in a glazing material<sup>21</sup>, the crystal phase of nanosized ZrO<sub>2</sub> is unclear; the content of ZrO<sub>2</sub> is low (up to 13.4 wt%; *cf.* The best mZrO<sub>2</sub> content was 73–91 wt% in this study); and the mechanical properties of glazed zirconia were not reported.

In this study, to understand the effect of heating temperature, the mZrO<sub>2</sub>/SiO<sub>2</sub>-coated PSZ treated at different heating temperatures (1,000, 1,300, or 1,500°C) were firstly evaluated at a constant mZrO<sub>2</sub>/SiO<sub>2</sub> ratio of 10/1. From the results, we found that higher heating temperature tended to increase the mechanical strength of PSZ. Therefore, to understand the effect of mZrO<sub>2</sub>/SiO<sub>2</sub> dispersion composition, the mZrO<sub>2</sub>/SiO<sub>2</sub>-coated PSZ treated at different mZrO<sub>2</sub>/SiO<sub>2</sub> weight ratio (20/1, 10/1, 8/3, or 6/5) were evaluated at a maximum heating temperature of 1,500°C. Of note, the heating temperature above 1,550°C, which is sintering temperature of pre-sintered PSZ in this study, was not applied because there is a risk of shrinkage or deformation of PSZ.

Strikingly, by this treatment, the mechanical strength of the treated samples increased up to 725 MPa. This value is almost 1.7 times higher than that of the original sample. The strength increased until the mZrO<sub>2</sub>/SiO<sub>2</sub> ratio was 10/1; however, the strength decreased when the SiO<sub>2</sub> content was higher than this ratio. This probably occurred because the mZrO<sub>2</sub> amount was the key factor underlying the improvement of the samples' mechanical properties. In addition, the higher content of SiO<sub>2</sub> seemed to decrease the presence of the mZrO<sub>2</sub> in its crystal structure, suggesting that (1) the tetragonal to monoclinic transformation upon cooling was prevented by SiO<sub>2</sub>, and that (2) Y<sup>3+</sup> near the PSZ substrate surface migrated into the coating layer at high temperatures. As for (1), mZrO<sub>2</sub> in the coating layer would transform into the tetragonal phase according to the phase transformation temperature (at ~1,200°C<sup>22,23</sup>), for high-temperature treatment at 1,300 and 1,500°C, whereas the monoclinic phase would not transform at

1,000°C. The tetragonal phase formed in the coating layer for temperatures above 1,300°C re-transformed upon cooling (at ~927°C<sup>24</sup>) into the monoclinic phase, with volume expansion that cause compression stress in the coating layer. However, it is known that the tetragonal phase can be stabilized without stabilizing ions such as Y<sup>3+</sup>, when the crystal size is sufficiently small (*e.g.*, 20 nm<sup>25</sup> and 45 nm<sup>26</sup>). Judging from the crystal size of ZrO<sub>2</sub> in the coating, the SiO<sub>2</sub> matrix prevented the crystal growth (or sintering) of mZrO<sub>2</sub> nanoparticles; hence, the tetragonal phase was still observed for high SiO<sub>2</sub> ratios. As for (2), a reaction between Y<sub>2</sub>O<sub>3</sub> and SiO<sub>2</sub> could occur above 1,000°C<sup>27</sup>, and the detached Y<sub>2</sub>O<sub>3</sub> from PSZ probably moved into the coating layer through the SiO<sub>2</sub> matrix to the stabilized tetragonal phase of ZrO<sub>2</sub> in the coating layer.

To understand the mechanisms of these phenomena, we conducted surface investigations using SEM and EDS. One of the important findings was that granule-like crystals were formed and grew on the surfaces of the mZrO<sub>2</sub>/SiO<sub>2</sub>-coated substrates. Interestingly, these granules packed together, and formed island-like patterns on the substrates' surfaces. These densely packed granules were observed up to the ratio of 8/3; however, the space between the granules in the islands became larger as the SiO<sub>2</sub> ratio increased beyond 8/3. Thus, the optimal mixing ratio of ZrO<sub>2</sub> and SiO<sub>2</sub> was estimated.

The major clinical problem with the use of zirconia-based ceramics is the difficulty in achieving suitable bonding to luting agents<sup>28-30</sup> or veneering/glazing ceramics<sup>31,32</sup>. The presence of SiO<sub>2</sub> on the coating layer would be preferable to achieve suitable bonding to luting agents/primers containing silane coupling agents and also to silica based veneering/glazing ceramics. Therefore, the mZrO<sub>2</sub>/SiO<sub>2</sub> coating method described here would be applicable for the superficies the zirconia crowns before veneering/glazing and also for the inside of the crowns in a dental laboratory process.

In recent years, many studies were conducted aiming to improve the mechanical strength of highly translucent PSZ<sup>8-10</sup>. Although our method improved the mechanical strength significantly, the resulting samples were still quite weak, compared with the strength of conventional Y-TZP molar crowns, ~1,200 MPa. Therefore, further improvement of the technique should be considered.

## CONCLUSION

The mechanical strength of highly translucent PSZ improved by 170% for the best condition, which was achieved by coating the samples with mZrO<sub>2</sub>/SiO<sub>2</sub> dispersion followed by heat treatment. This technique is a promising method for improving the mechanical properties of highly translucent PSZ.

## REFERENCES

- 1) Luthardt RG, Holzhüter M, Sandkuhl O, Herold V, Schnapp JD, Kuhlisch E, *et al.* Reliability and properties of ground

- Y-TZP-zirconia ceramics. *J Dent Res* 2002; 81: 487-491.
- 2) Jeong SM, Ludwig K, Kern M. Investigation of the fracture resistance of three types of zirconia posts in all-ceramic post-and-core restorations. *Int J Prosthodont* 2002; 15: 154-158.
  - 3) Chevalier J, Grenmillard L, Virkar AV, Clarke DR. The tetragonal-monoclinic transformation in zirconia: lessons learned and future trends. *J Am Ceram Soc* 2009; 92: 1901-1920.
  - 4) Pereira GK, Silvestri T, Camargo R, Rippe MP, Amaral M, Kleverlaan CJ, *et al.* Mechanical behavior of a Y-TZP ceramic for monolithic restorations: effect of grinding and low-temperature aging. *Mater Sci Eng C Mater Biol Appl* 2016; 63: 70-77.
  - 5) Matsui K, Yamakawa T, Uehara M, Enomoto N, Hojo J. Mechanism of alumina-enhanced sintering of fine zirconia powder: Influence of alumina concentration on the initial stage sintering. *J Am Ceram Soc* 2008; 91: 1888-1897.
  - 6) Mao L, Kaizer MR, Zhao M, Guo B, Song YF, Zhang Y. Graded ultra-translucent zirconia (5Y-PSZ) for strength and functionalities. *J Dent Res* 2018; 97: 1222-1228.
  - 7) Inokoshi M, Shimizu H, Nozaki K, Takagaki T, Yoshihara K, Nagaoka N, *et al.* Crystallographic and morphological analysis of sandblasted highly translucent dental zirconia. *Dent Mater* 2018; 34: 508-518.
  - 8) Zhang F, Inokoshi M, Batuk M, Hadermann J, Naert I, Van Meerbeek B, *et al.* Strength, toughness and aging stability of highly-translucent Y-TZP ceramics for dental restorations. *Dent Mater* 2016; 32: e327-337.
  - 9) Nakamura T, Nakano Y, Usami H, Wakabayashi K, Ohnishi H, Sekino T, *et al.* Translucency and low-temperature degradation of silica-doped zirconia: A pilot study. *Dent Mater J* 2016; 35: 571-577.
  - 10) Toyama DY, Alves LMM, Ramos GF, Campos TMB, de Vasconcelos G, Borges ALS, *et al.* Bioinspired silica-infiltrated zirconia bilayers: Strength and interfacial bonding. *J Mech Behav Biomed Mater* 2019; 89: 143-149.
  - 11) Promakhov V, Kulkov N. Thermal expansion of oxide systems on the basis of ZrO<sub>2</sub>. *J Silic Based Compos Mater* 2014; 66: 81-83.
  - 12) Hayashi H, Saitou T, Maruyama N, Inaba H. Thermal expansion coefficient of yttria stabilized zirconia for various yttria contents. *Solid State Ion* 2005; 176: 613-619.
  - 13) Ezo M, Murase Y, Daimon K, Kato E. Formation and thermal change of monoclinic zirconia polycrystalline thin films by Sol-Gel process. *Yogyo-Kyokaiishi* 1986; 94: 823-826.
  - 14) Murase Y, Kato E. Preparation of zirconia whiskers from zirconium hydroxide in sulfuric acid solutions under hydrothermal conditions at 200°C. *J Am Ceram Soc* 2001; 84: 2705-2706.
  - 15) Wille S, Zumstrull P, Kaidas V, Jessen LK, Kern M. Low temperature degradation of single layers of multilayered zirconia in comparison to conventional unshaded zirconia: Phase transformation and flexural strength. *J Mech Behav Biomed Mater* 2018; 77: 171-175.
  - 16) Pecho OE, Ghinea R, Ionescu AM, Cardona Jde L, Paravina RD, Pérez Mdel M. Color and translucency of zirconia ceramics, human dentine and bovine dentine. *J Dent* 2012; 40: e34-40.
  - 17) Johnston WM, Ma T, Kienle BH. Translucency parameter of colorants for maxillofacial prostheses. *Int J Prosthodont* 1995; 8: 79-86.
  - 18) Miyazaki T, Nakamura T, Matsumura H, Ban S, Kobayashi T. Current status of zirconia restoration. *J Prosthodont Res* 2013; 57: 236-261.
  - 19) Hoydalsvik K, Barnardo T, Winter R, Haas S, Tatchev D, Hoell A. Yttria-zirconia coatings studied by grazing-incidence small-angle X-ray scattering during in situ heating. *Phys Chem Chem Phys* 2010; 12: 14492-14500.
  - 20) Ryan DPO, Fais LMG, Antonio SG, Hatanaka GR, Candido LM, Pinelli LAP. Y-TZP zirconia regeneration firing: Microstructural and crystallographic changes after grinding. *Dent Mater J* 2017; 36: 447-453.
  - 21) Venkatesh G, Thenmuhil D, Vidyavathy SM, Vinothan R. Effect of addition of nano zirconia in ceramic glazes. *Adv Mater Res* 2014; 984-985: 488-494.
  - 22) Kuwabara A, Tohei T, Yamamoto T, Tanaka I. Ab initio lattice dynamics and phase transformations of ZrO<sub>2</sub>. *Phys Rev B* 2005; 71: 064301.
  - 23) Patil RN, Subbarao EC. Axial thermal expansion of ZrO<sub>2</sub> and HfO<sub>2</sub> in the range room temperature to 1400°C. *J Appl Crystallogr* 1969; 2: 281-288.
  - 24) Subbarao EC, Maiti HS, Srivastava KK. Martensitic transformation in zirconia. *Phys Status Solidi* 1974; 21: 9-40.
  - 25) Wu NL, Wu TF. Thermodynamic stability of tetragonal zirconia nanocrystallites. *J Mater Res* 2001; 16: 666-669.
  - 26) Shukla S, Seal S, Vij R, Bandyopadhyay S, Rahman Z. Effect of nanocrystallite morphology on the metastable tetragonal phase stabilization in zirconia. *Nano Lett* 2002; 2: 989-993.
  - 27) Ahlawat R, Aghamkar P. Influence of annealing temperature on Y<sub>2</sub>O<sub>3</sub>:SiO<sub>2</sub> nanocomposite prepared by sol-gel process. *Acta Phys Pol A* 2014; 126: 736-739.
  - 28) Thompson JY, Stoner BR, Piascik JR, Smith R. Adhesion/cementation to zirconia and other non-silicate ceramics: where are we now? *Dent Mater* 2011; 27: 71-82.
  - 29) Tzanakakis E-GC, Tzoutzas IG, Koidis PT. Is there a potential for durable adhesion to zirconia restorations? A systematic review. *J Prosthet Dent* 2016; 115: 9-19.
  - 30) Okada M, Inoue K, Irie M, Taketa H, Torii Y, Matsumoto T. Resin adhesion strengths to zirconia ceramics after primer treatment with silane coupling monomer or oligomer. *Dent Mater J* 2017; 36: 600-605.
  - 31) Kim HJ, Lim HP, Park YJ, Vang MS. Effect of zirconia surface treatments on the shear bond strength of veneering ceramic. *J Prosthet Dent* 2011; 105: 315-322.
  - 32) Miyazaki T, Nakamura T, Matsumura H, Ban S, Kobayashi T. Current status of zirconia restoration. *J Prosthodont Res* 2013; 57: 236-261.